tion Biology and Evolution of Clonal Organisms, J. B. C. Jackson, L. W. Buss, R. E. Cook, Eds. (Yale Univ. Press, New Haven, CT, 1985), pp. 297–355.
10. W. C. Banta *et al.*, *Science* **185**, 783 (1974).
11. J. E. Winston, *Bull. Mar. Sci.* **28**, 1 (1978).
12. ——, in *Advances in Bryozoology*, G. P. Larwood and M. B. Abbott, Eds. (Academic Press, London, 1979), pp. 247–267.
13. F. K. McKinney, *Am. Nat.* **128**, 795 (1986).
14. ——, *Rev. Aquatic Sci.*, in press.
15. J. E. Winston, in *Biology of Bryozoans*, R. M. Woollacott and R. L. Zimmer, Eds. (Academic Press, New York, 1977), pp. 233–271.
16. F. Borg, *Zool. Bidr. Upps.* **10**, 181 (1926).
17. J. S. Bullivant, *N.Z. J. Mar. Freshwater Res.* **2**, 135 (1968).
18. Unwanted particles, including those too large to ingest, are passed by various rejection or avoidance behaviors through lophophores of bryozoans into the colonial current system or are bounced along tops of lophophores to nearest chimneys [(*11, 12*); F. K. McKinney, personal observation].
19. S. M. Stanley, B. V. Valkenburg, R. S. Steneck, in *Coevolution*, D. J. Futuyma and M. Slatkin, Eds. (Sinauer Associates, Sunderland, MA, 1983), pp. 328–349.
20. G. J. Vermeij, in *ibid.*, pp. 311–327.
21. J. L. Wulff, in *Population Biology and Evolution of Clonal Organisms*, J. B. C. Jackson, L. W. Buss, R. E. Cook, Eds. (Yale Univ. Press, New Haven, CT, 1985), pp. 437–466.
22. Although *Aulopora* and *Leioclema* were not originally members of the same guild, they did compete for a shared and distinctly limited resource, substrate space.
23. R. W. Osman and J. A. Haugsness, *Science* **211**, 846 (1981); H. Ristedt and H. Schumacher, *Mar. Ecol.* **6**, 167 (1985); F. K. McKinney, personal observation.
24. A. R. D. Stebbing, in *Living and Fossil Bryozoa*, G. P. Larwood, Ed. (Academic Press, London, 1973), pp. 173–183; G. M. Wellington, *Oecologia (Berlin)* **47**, 340 (1980); L. W. Buss, in *Recent and Fossil Bryozoa*, G. P. Larwood and C. Nielsen, Eds. (Olsen & Olsen, Fredensborg, Denmark, 1981), pp. 39–49; R. P. M. Bak, R. M. Termaat, R. Dekker, *Mar. Biol.* **69**, 215 (1982).

25. We thank R. Dewel for assistance in the Appalachian State University Electron Microscopy Laboratory, M. McKinney for photography, and J. B. C. Jackson and M. Foote for discussion and criticism.

7 November 1989; accepted 13 February 1990

Twinning in $MgSiO_3$ Perovskite

YANBIN WANG, FRANCOIS GUYOT, AMIR YEGANEH-HAERI,
ROBERT C. LIEBERMANN

Crystals of $MgSiO_3$ perovskite synthesized at high pressures and temperatures have orthorhombic symmetry under ambient conditions. Examination by transmission electron microscopy shows that the microstructure of crystals synthesized at 26 gigapascals and 1600°C is dominated by a large number of twin domains that are related by reflection operations with respect to {112} and {110} planes. These twins may be associated with the transformations of $MgSiO_3$ perovskite from the cubic to tetragonal and tetragonal to orthorhombic phases, respectively, upon decreasing pressure and temperature. These observations suggest that under the experimental synthesis conditions, and perhaps in the earth's lower mantle, the stable phase of $MgSiO_3$ might have the cubic perovskite structure.

MANY MATERIALS WITH ABX_3 compositions and perovskite-type structures undergo sequences of crystallographic phase transitions (*1*) from high- to low-symmetry forms on decreasing temperature, for example, $SrTiO_3$ (*2*), $CsPbCl_3$ (*3*), $NaMgF_3$ (*4*), and $CaTiO_3$ (*5*). These transitions are commonly associated with dramatic changes in magnetic, electric, thermal, and elastic properties and thus are of great interest in materials science and condensed matter physics. Optical and electron microscopy studies indicate that twinning is the predominant microstructural feature in the lower symmetry polymorphs of these perovskites, and the presence of these twins may have important consequences for the physical properties of these materials (*6*).

High-pressure, high-temperature experiments suggest that (Mg,Fe)SiO_3 perovskite is the dominant phase of the earth's lower mantle [pressures above 23 gigapascals (GPa) and depths of 670 to 2900 km (*7*)] and, therefore, probably the most abundant mineral of our planet. X-ray diffraction studies of specimens recovered from the experiments have revealed that at ambient conditions the crystal structure is orthorhombic (space group *Pbnm*) and isostructural with the $GdFeO_3$ structure (*8*); these specimens have also been studied by vibrational spectroscopy (*9*), x-ray absorption spectroscopy (*10*), electron diffraction (*11*), and high-resolution electron microscopy (*12*). Most of these analyses have been performed under conditions at which $MgSiO_3$ perovskite is thermodynamically metastable. Under laser irradiation (*9*) or heating above 150°C (*13*) at 1 bar, single crystals have been observed to twin and then rapidly to amorphize. Application of nonhydrostatic stress also can cause twinning in single crystals (*14*). In this report, we characterize the observed twin laws in $MgSiO_3$ perovskite by transmission electron microscopy (TEM) and discuss the implications of twinning for the physical behavior and possible polymorphism of perovskite in the mantle.

We synthesized polycrystalline specimens of $MgSiO_3$ perovskite (0.9 mm in diameter and 1.5 mm in length) from enstatite powder starting material in a 2000-ton uniaxial split-sphere apparatus (USSA-2000) (*15*) following cell designs and techniques developed by Ito and Weidner (*16*) but without adding water to the capsule. Samples were elevated to 26 GPa and 1600°C for 0.5 to 2 hours and either quenched immediately or cooled to 1200°C at a rate of 30°C per minute before quenching. Thin foils were prepared by Ar ion-milling of thin sections (*17*) for observation in a JEOL 200CX transmission electron microscope that was operated at 200 kV. Electron diffraction confirmed that the recovered $MgSiO_3$ perovskite is isostructural with $GdFeO_3$ (space group *Pbnm*). The lattice dimensions are

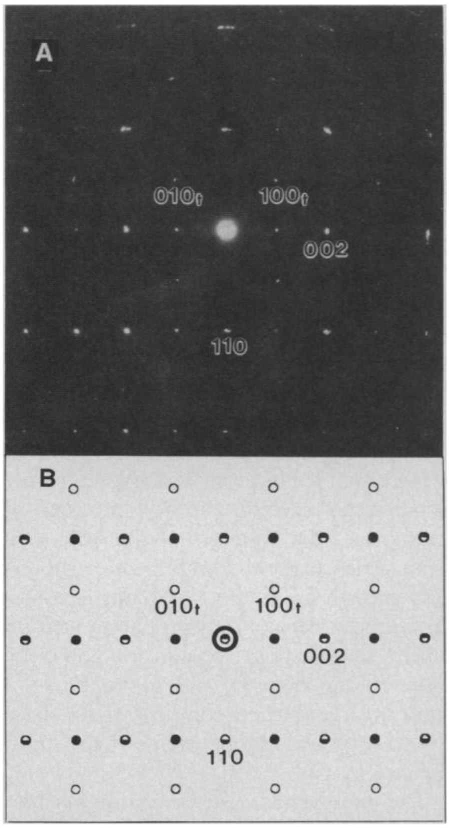

Fig. 1. (**A**) Selected-area electron diffraction (SAED) pattern of $MgSiO_3$ perovskite showing $(\bar{1}12)$ twinning. Diffraction spots (100_t and 010_t) corresponding to the twinned (t) crystal are indicated. (**B**) Schematic of diffraction pattern in (A). Solid circles are diffraction spots from a single crystal domain; open circles are spots attributed to $(\bar{1}12)$ twinning. Patterns viewed along the $[1\bar{1}0]$ zone axis of the matrix (solid spots). Half-filled symbols represent overlapping spots.

Mineral Physics Institute, Earth and Space Sciences Building, State University of New York at Stony Brook, Stony Brook, NY 11794.

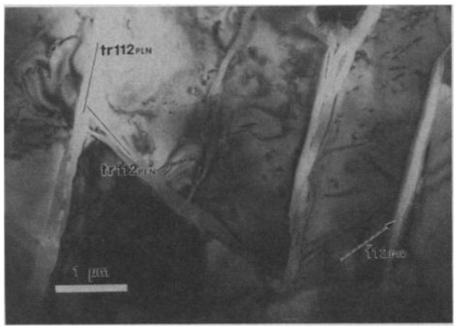

Fig. 2. Electron micrograph of $MgSiO_3$ perovskite showing {112} twin domains, viewed along the [02$\bar{1}$] zone axis. The trace (tr) of two planes (PLN) are indicated; all the twin boundaries are {112} type. Narrow twin domains amorphized at a faster rate than did the matirx, which is now strained after the amorphization process. Note also the straight fringes in the [$\bar{1}$12] direction (DIR) at lower right. Sample quenched from 1200°C.

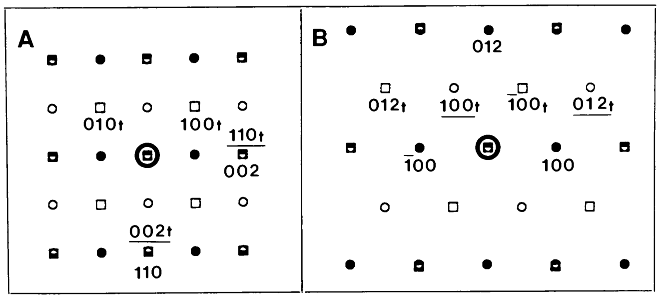

Fig. 3. Theoretical diffraction patterns of coexisting (112) and ($\bar{1}$12) twins. Solid circles are spots of the matrix, open circles due to (112) twinning and open squares due to ($\bar{1}$12) twinning. (**A**) and (**B**) are patterns viewed along the [1$\bar{1}$0] ([010]$_{pc}$) and [02$\bar{1}$] ([1$\bar{1}\bar{1}$]$_{pc}$) zone axes, respectively, of the matrix (pc, pseudocubic). In both cases the whole pattern shows an apparent cubic symmetry [spots form square array in (A) and hexagonal array in (B)], and thus may be indexed as a cubic structure with a unit cell dimension of 6.9 Å. Compare with figures 2 and 4A of Madon *et al.* (*12*).

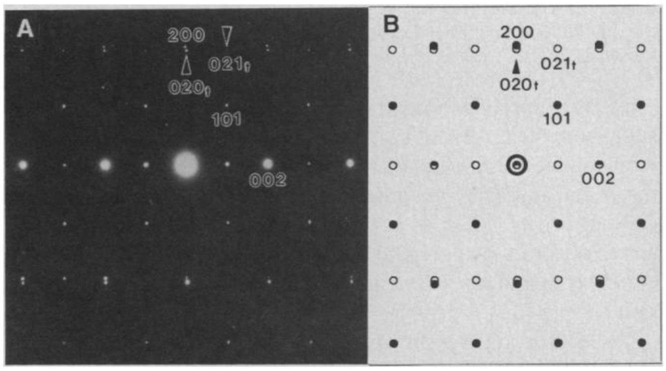

Fig. 4. (**A**) SAED pattern showing (110) twinning. Notice coexisting 021_t- and 101-type spots and splitting of the 200- and 020_t-type and 202- and 022_t-type spots. (**B**) Schematic of diffraction pattern in (A). Solid circles diffraction are spots from a single crystal domain; open circles are spots due to (110) twinning.

consistent with earlier x-ray cyrstallographic analyses, that is, *a* is 4.78, *b* is 4.93, and *c* is 6.90 Å (*8*).

All of the crystals contained numerous twin domains. The twinned crystals produced electron diffraction patterns that appear to be inconsistent with the *Pbnm* space group because of the presence of an additional set of diffraction spots that are generated by a mirror operation across the ($\bar{1}$12) plane (Fig. 1). Twinning also has developed elsewhere on other symmetrically equivalent {112} planes, for instance (112) and (1$\bar{1}$2).

In general (Fig. 2), the {112} twins appear as lamellar features parallel to the (112) and ($\bar{1}$12) planes (*18*). Twin boundaries (that is, domain walls) are somewhat distorted but mostly parallel to low-index crystallographic planes [{112}, {110}, (100) or (010), and (001)]. Symmetrically equivalent {112} twin domains commonly occur together in the same area and intersect at 120° (Fig. 2).

Theoretical patterns of the {112} twins (Fig. 3) accurately reproduce diffraction patterns observed by Madon *et al* (*11*) in $Mg_{0.93}Fe_{0.07}SiO_3$ perovskite. Thus, our results confirm the suggestion that this twinning is the cause of the apparent doubling of the unit cell of the (Mg,Fe)SiO_3 perovskite (*21*).

Twinning on {110} planes results from the interchange of the *a* and *b* axes (Fig. 4). In $MgSiO_3$ perovskite, the orthorhombic distortion from tetragonal symmetry is sufficiently large ($a/b = 0.969$, significantly different from 1) that the individual spots resulting from this interchange can be clearly observed. The resultant pattern (Fig. 4A) is identical to that calculated (Fig. 4B) by reflection with respect to the (110) plane.

Domain walls for the {110} twins are generally {110} planes that intersect to form right-angled domains (Fig. 5). Theoretically, the curvature of the domain walls near the domain corners (see arrows in Fig. 5) can be used to provide a measure of elastic constants of the material (*19*). The curvature of the twin walls suggests stress release during their formation (*19*), which could have been a consequence of either transformational or deformational processes; therefore, {110} twins are most likely formed during cooling and unloading, not during growth.

Similar twinning has also been found in several other materials isostructural with $MgSiO_3$ perovskite. The {110}-type twins have been the most commonly observed [for example, in $CsPbCl_3$ (*6*), rare-earth titanates and ferrites (*22*), and in the high-pressure phases of $CaGeO_3$ and $MnGeO_3$ produced in a large-volume apparatus or diamond-anvil cell (*20*)]. The {112}-type twins have been observed in $CsPbCl_3$ (*6*), $LaTiO_3$ (*22*), and $CaTiO_3$, $CaGeO_3$, and $MnGeO_3$ [(*20*); also see (*23*)]. These {112} reflection twins have often been described as rotation twins. For $CaTiO_3$, however, two of the three twin relations (*23*) [namely the twins that have been previously described by a 90° rotation about the normal to (110) and by a 180° rotation about the normal to (112)] are unequivocally {112} reflection twins.

The occurrence of the {112} and {110} twins is a direct consequence of structural distortions in $MgSiO_3$ perovskite relative to the "ideal" perovskite structure. In the idealized structure, eight corner-sharing SiO_6 octahedra form a cubic framework, and the Mg cations are located in the central dodecahedral cavities (Fig. 6A). The structure is cubic (space group *Pm3m*); $a_c \approx 3.5$ Å (c refers to a cubic unit cell). At ambient conditions, $MgSiO_3$ perovskite is distorted from cubic, but because the distortion is slight, the orthorhombic structure has a pseudotetragonal ($a \approx b \approx \sqrt{2}a_c$) and a pseudocubic symmetry ($c \approx 2a_c$).

The orthorhombic distortion can be described by two tilts of the SiO_6 octahedra from the ideal cubic structure (*24*). The first is a rotation of the octahedra by a small angle about the $[001]_c$ axis. Each parallel string of octahedra along the $[001]_c$ axis is rotated by the same angle, and adjacent strings are rotated in the opposite sense (Fig. 6B). The originally perfect cube becomes a pseudocube (pc), and the structure has tetragonal symmetry (tetr; space group *P4/mbm*). Such a tilt can take place along any of the three $<100>_c$-type axes. In the tetragonal phase, any two adjacent domains resulting from tilts about two perpendicular axes (say, $[100]_c$ and $[001]_c$), are related by a reflection operation [for example, across the $(101)_c$ plane, which is equivalent to the $(111)_{tetr}$ plane, or approximately the (112) orthorhombic plane]. This reflection operation is one of the symmetry elements lost during a transition from cubic to tetragonal symmetry. Twinning can form on three symmetrically equivalent {112} planes be-

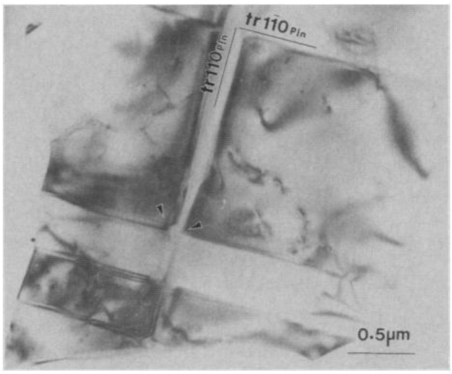

Fig. 5. Representative {110} twin domains with (110) and ($1\bar{1}0$) domain boundaries. Notice the distortion (curvature) of the twin boundaries near the domain corners (arrowheads). Same sample as shown in Fig. 2.

cause there are three potential axes of tilt in a cubic unit cell. When two twin relations with independent twin planes are present, the crystal aggregate possesses reflection operations across {112}; as a result, diffraction patterns from the aggregate show an apparent cubic symmetry (see Fig. 3 and discussion above).

The second tilt is a similar rotation along $[110]_{pc}$ (Fig. 6C). The new pseudocubic axes become nonorthogonal and the fourfold symmetry in the $(001)_{tetr}$ plane is replaced by twofold symmetry. The structure becomes orthorhombic (space group *Pbnm*). This type of tilt can also take place about the $[1\bar{1}0]_{pc}$ axis. Any two adjacent domains that result from tilts about the $[110]_{pc}$ and $[1\bar{1}0]_{pc}$ axes are related by a reflection across the $(100)_{pc}$ plane, which is equivalent to the $(110)_{tetr}$ plane and approximately the orthorhombic (110) plane. Because there are two potential tilt axes in a tetragonal unit cell, there are two symmetrically equivalent {110} twins, namely those on $(110)_{tetr}$ and $(1\bar{1}0)_{tetr}$ (*25*).

All distorted perovskites should eventually transform to the ideal cubic structure on increasing temperature, provided that melting or decomposition does not occur before the transition. Polymorphism in perovskite-structure materials is almost inevitably associated with twinning (*7, 22*). In $CsPbCl_3$ (*7*), the {110} twinning has been ascribed to a transition from tetragonal to orthorhombic symmetry. The {112} twins in $CsPbCl_3$ perovskite are not affected by heating through the orthorhombic-tetragonal transition, but they disappear at temperatures above the tetragonal-cubic transition; this pattern is consistent with our geometrical interpretations of the {112} twinning. When $CaTiO_3$ perovskite is heated above its orthorhombic-tetragonal transition (*5*) and then cooled down to room temperature, the density of {110} twins increases dramatically (*20*). High-temperature TEM study of $NaNbO_3$ perovskite has shown that the {112} and {110} twins are associated with cubic-tetragonal and tetragonal-orthorhombic transitions, respectively (*27*).

By analogy with these isostructural materials, we suggest that the {112} and {110} twins observed in our specimens of orthorhombic $MgSiO_3$ perovskite are associated with the transformations from cubic to tetragonal and tetragonal to orthorhombic symmetry, respectively. Theoretically, these transitions should produce domain walls in a limited number of "permissible" orientations (*27*), which are consistent with our experimental findings in $MgSiO_3$ perovskite. Moreover, TEM observations on analog perovskites (*20, 26*) indicate that twin walls induced by phase transitions are morphologically different from those induced by deformation; deformation twins are preferentially oriented because of the presence of nonhydrostatic stress and irregular in shape because of interactions with dislocations and stacking faults. Furthermore, the increase of twin density with quench temperature (*18*) makes it unlikely that the twins are produced by growth or deformation.

The observed {112} and {110} twins and microstructures therefore suggest that under the synthesis conditions (26 GPa, 1600°C), $MgSiO_3$ was within or close to the cubic perovskite stability field. This inference is supported by the theoretical calculations of Wolf and Bukowinski (*28*), who have computed the stability fields for the orthorhombic, tetragonal, and cubic $MgSiO_3$ perovskite polymorphs. Because these laboratory conditions are comparable to those estimated for depths of about 750 km in the earth's interior, our data imply that cubic $(Mg,Fe)SiO_3$ perovskite may be the dominant mineralogical phase in the lower mantle.

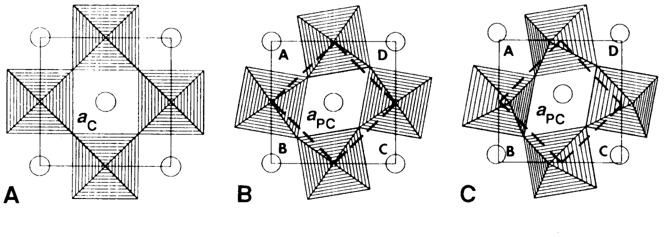

Fig. 6. (**A**) The ideal cubic perovskite structure viewed along $[001]_c$. Open circles are Mg atoms; Si and O are not shown individually but are represented by SiO_6 octahedra. Unit cell with dimension a_c is defined by middle points of the four octahedra. (**B**) Tilting of SiO_6 octahedra about $[001]_c$. Tetragonal unit cell is defined by square ABCD. The perfect cube in (A) becomes a pseudocube (dashed square), the dimensions of which in the plane are a_{pc}, slightly shorter than the third dimension c_{pc}, which equals a_c. (**C**) Tilting of octahedra about the $[110]_{pc}$ axis [vertical diagonal of dashed square in (B)]; Mg atoms are displaced accordingly. Orthorhombic (orth) unit cell is still ABCD, which is now a rectangle with BC (a_{orth}) slightly shorter than AB (b_{orth}). The third dimension of the unit cell is doubled, $c_{orth} \approx 2a_c$. Other layers can be generated by a mirror plane parallel to the page. Atomic displacements are not drawn to scale.

REFERENCES AND NOTES

1. A. M. Glazer, *Acta Crystallogr. Sect. B* **28**, 3384 (1972); K. S. Aleksandrov, *Ferroelectrics* **14**, 801 (1976); *ibid.* **20**, 61 (1978).
2. G. Rupprecht and W. H. Winter, *Phys. Rev.* **155**, 1019 (1967).
3. S. Hirotsu and T. Suzuki, *J. Phys. Soc. Jpn.* **44**, 1604 (1978).
4. E. C. Chao, H. T. Evans, B. J. Skinner, C. Milton, *Am. Mineral.* **46**, 379 (1961).
5. X. Liu and R. C. Liebermann, in preparation.
6. $BaTiO_3$, V. C. S. Prasad and E. C. Subbarao, *Ferroelectrics* **15**, 143 (1977); $CsPbCl_3$, S. Horitsu, *J. Phys. Soc. Jpn.* **31**, 552 (1971); $KNaO_3$, E. Wiesendanger, *Czech. J. Phys.* **B23**, 91 (1973).
7. L. G. Liu, *Geophys. Res. Lett.* **2**, 417 (1975); E. Knittle and R. Jeanloz, *Science* **235**, 669 (1987).
8. H. Horiuchi, E. Ito, D. J. Weidner, *Am. Mineral.* **72**, 357 (1987); see also E. Ito and Y. Matsui, *Earth Planet. Sci. Lett.* **38**, 435 (1978).
9. Q. Williams, R. Jeanloz, P. McMillan, *J. Geophys. Res.* **92**, 8116 (1987); A. Yeganeh-Haeri, D. J. Weidner, E. Ito, in *Perovskite: A Structure of Great Interest to Geophysics and Materials Science*, A. Navrotsky and D. J. Weidner, Eds. (American Geophysical Union, Washington, DC, 1989), pp. 13–25; R. J. Hemley, R. E. Cohen, A. Yeganeh-Haeri, H. K. Mao, D. J. Weidner, E. Ito, in *ibid.*, pp. 35–44.
10. W. E. Jackson, E. Knittle, G. E. Brown, R. Jeanloz, *Geophys. Res. Lett.* **14**, 224 (1987).
11. M. Madon, P. M. Bell, H. K. Mao, J. P. Poirier, *ibid.* **7**, 629 (1980).
12. I. Hassan, Y. Kudoh, P. R. Buseck, E. Ito, *Eos* **69**, 1436 (1988).
13. N. L. Ross and R. M. Hazen, *Phys. Chem. Minerals* **16**, 415 (1989).
14. Y. Kudoh, G. H. Wolf, P. K. Buseck, H. Takeda, E. Ito, in preparation.
15. A. R. Remsberg, J. N. Boland, T. Gasparik, R. C. Liebermann, *Phys. Chem. Minerals* **15**, 498 (1988); T. Gasparik, *Contrib. Mineral. Petrol.* **102**, 389 (1989).
16. E. Ito and D. J. Weidner, *Geophys. Res. Lett.* **13**, 464 (1986).
17. The high-energy ion beam amorphized almost completely the metastable perovskite crystals, probably because of the build-up of temperature during ion bombardment. On the basis of estimates given by D. J. Barber [*J. Mater. Sci.* **5**, 3 (1970)], the sample temperature would have been about 150°C during ion thinning. Sample stability was much improved when a low-tension, low-current Ar beam was used. The thinned foils were then coated with C on both sides to minimize temperature buildup under the electron beam.
18. In the specimens that were cooled slowly to 1200°C, twin lamellae are approximately 0.1 to 0.2 µm in width and have a typical separation of ~1 µm; twin lamellae are much finer in the specimens quenched from 1600°C. These lamellae amorphized at a faster rate than did the matrix; those in Fig. 2 have almost completely amorphized within 1 minute.
19. N. Yamamoto, K. Yagi, G. Honjo, *Phys. Stat. Solidi A* **41**, 523 (1977); *ibid.* **42**, 257 (1977); J. Torres, C. Roucan, R. Ayroles, *ibid.* **70**, 659 (1982); *ibid.*, p. 193; E. Salje, B. Kuscholke, B. Wruck, *Phys. Chem. Minerals* **12**, 132 (1985).
20. Y. Wang, F. Guyot, R. C. Liebermann, in preparation.
21. M. Madon, F. Guyot, J. Peyronneau, J. P. Poirier, *Phys. Chem. Minerals* **16**, 320 (1989).

22. D. A. Maclean, H.-N. Ng, J. E. Greedan, *J. Solid State Chem.* **30**, 35 (1979); M. Marezio, J. P. Remeika, P. D. Dernier, *Acta Crystallog. Sect. B* **26**, 300 (1970).
23. H. B. Bowman, *Mineral. Mag.* **15**, 156 (1908); T. J. White, R. L. Segall, J. C. Barry, J. L. Hutchison, *Acta Cryst.* **B41**, 93 (1985).
24. H. D. Megaw, *Crystal Structures: A Working Approach* (Saunders, Philadelphia, 1973).
25. The sequence of phase transitions (*Pm3m* to *P4/mbm* to *Pbnm*) is somewhat arbitrary and chosen only for convenience. In the transition from *Pm3m* to *Pbnm*, there are a limited number of possible intermediate structures [see (*1*)]. Our conclusions hold for the general transition sequence (in terms of point group symmetry) from *m3m* to *4/mmm* to *mmm*.
26. In situ high-temperature TEM study on structural phase transitions in $NaNbO_3$ has shown that the two twin-types, {141} and {101} (equivalent to the {112} and {110} twinning, respectively, in $MgSiO_3$), are consistent with our geometrical interpretation and are associated with cubic-tetragonal and tetragonal-orthorhombic transitions, respectively; F. Guyot and Y. Wang, in preparation.
27. For the transition from cubic to tetragonal (*Pm3m* to *P4/mbm*), theory [J. Sapriel, *Phys. Rev. B* **12**, 5128 (1975)] predicts that there are three possible twin relations and six permissible domain wall orientations: $(110)_c$, $(011)_c$, $(101)_c$, $(\bar{1}01)_c$, $(1\bar{1}0)_c$, and $(10\bar{1})_c$. These are approximately either (100), (010), or {112} planes in the orthorhombic structure. For the transition from tetragonal to orthorhombic (*P4/mbm* to *Pbnm*), there are two possible twin relations and two permissible domain wall orientations $\{110\}_{tetr}$ (approximately orthorhombic {110}).
28. G. H. Wolf and M. S. T. Bukowinski, in *High-Pressure Research in Mineral Physics* (Akimoto volume), M. H. Manghnani and Y. Syono, Eds. (American Geophysical Union, Washington, DC, 1987), pp. 313–331.
29. We thank T. Gasparik and D. J. Weidner for advice on cell assemblies and X. Liu, Y. Kudoh, J. P. Poirier, R. J. Reeder, E. Salje, and D. J. Weidner for stimulating discussions. We also thank D. Presnall for the enstatite starting material and Y. Kudoh for a preprint of (*14*). The High-Pressure Laboratory is supported by the National Science Foundation (NSF) grant EAR 86-07105 and the State University of New York at Stony Brook. The electron microscopy was performed with the use of a JEOL 200CX transmission electron microscope under the supervision of R. J. Reeder. The research was also supported by NSF grants EAR 88-17097 and 88-04087.

16 November 1989; accepted 23 March 1990

GT-1 Binding Site Confers Light Responsive Expression in Transgenic Tobacco

ERIC LAM* AND NAM-HAI CHUA

Light-dependent expression of *rbcS*, the gene encoding the small subunit of ribulose-1,5-bisphosphate carboxylase, which is the key enzyme involved in carbon fixation in higher plants, is regulated at the transcriptional level. Sequence analysis of the gene has uncovered a conserved GT motif in the −150 to −100 region of many *rbcS* promoters. This motif serves as the binding site of a nuclear factor, designated GT-1. Analysis of site-specific mutants of pea *rbcS-3A* promoter demonstrated that GT-1 binding in vitro is correlated with light-responsive expression of the *rbcS* promoter in transgenic plants. However, it is not known whether factors other than GT-1 might also be required for activation of transcription by light. A synthetic tetramer of box II (TGTGTGGTTAATATG), the GT-1 binding site located between −152 to −138 of the *rbcS-3A* promoter, inserted upstream of a truncated cauliflower mosaic virus 35*S* promoter is sufficient to confer expression in leaves of transgenic tobacco. This expression occurs principally in chloroplast-containing cells, is induced by light, and is correlated with the ability of box II to bind GT-1 in vitro. The data show that the binding site for GT-1 is likely to be a part of the molecular light switch for *rbcS* activation.

THE ELUCIDATION OF THE MOLECULAR mechanisms for light-responsive gene expression is an important step toward understanding photomorphogenesis. While the mechanism by which the photoreceptor phytochrome transmits its signal remains unknown, analyses of light-regulated genes in transgenic plants have demonstrated that the promoter region of many of these genes harbors DNA elements for light-responsive expression (*1, 2*). In addition, the promoters of several *rbcS* (genes that encode the small subunit of ribulose-1,5-bisphosphate carboxylase) direct expression preferentially in chloroplast-containing cells (*3, 4*). Thus, the promoter for *rbcS* contains genetic information for light responsiveness as well as for cell specificity. In vitro studies with plant nuclear extracts have identified GT-1 (*5*) and a G-box factor (*6*) as nuclear proteins that interact with light-responsive promoters. The binding of GT-1 has been mapped to conserved elements termed box II and box III in the upstream regions of *rbcS* promoters from many dicotyledonous species (*1, 5*). Site-specific mutations in box II and box III result in a loss of GT-1 binding in vitro and are correlated with the attenuation of the *rbcS-3A* promoter function in vivo (*7*). In addition, a 116–base pair (bp) fragment, from −166 to −50 of *rbcS-3A*, containing box II (5′-GTGTGGTTAATATG-3′) and box III (5′-ATCATTTTCACT-3′), is able to confer light responsiveness to the cauliflower mosaic virus (CaMV) 35*S* promoter truncated at −46 (*8*). These studies show that GT-1 binding is likely to be necessary for the light-dependent activation process under our assay conditions. However, whether GT-1 alone is sufficient or binding of additional factors to the 116-bp fragment is also required for light-responsive gene

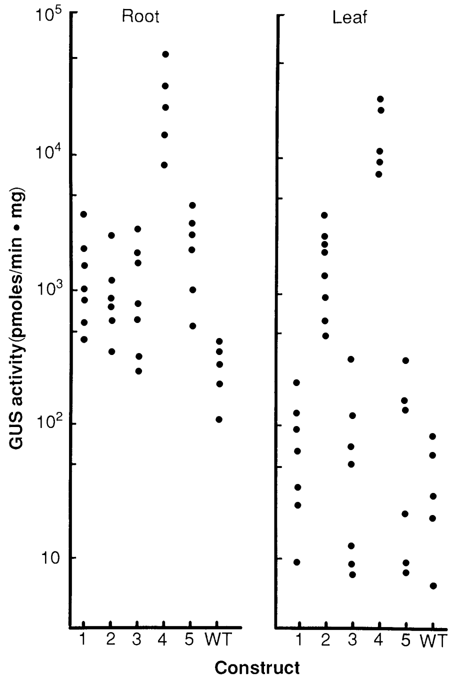

Fig. 1. Activity of *rbcS-3A* box II and *as-1* tetramers in transgenic tobacco. Activity is expressed as picomoles of 4-methylumbelliferone produced per minute per milligram protein, with 4-methyl umbelliferyl glucuronide as substrate (*15*). Data from five to ten independent transgenic plants for each construct are shown. *RbcS-3A* box II sequence (−152 to −138) is TGTGTGGTTAATATG and its mutant sequence is TGTGTCCTTAATATG, with the mutated bases underlined (*12*). Activation sequence-1 (*as-1*) is derived from the −82 to −62 region of the CaMV 35*S* promoter upstream sequence and has the sequence CTGACGTAAGGGATGACGCAC. The sequence of its mutant derivative is CTGCTGTAAGGGATCTCGCAC, with the mutated bases underlined (*13*). Tetramers of box II and its mutant derivative are designated 4II and 4IIm, respectively. Tetramers of *as-1* and its mutant derivative are designated 4AS1 and 4AS1m, respectively. All tetramers were synthesized with a Hind III site on the 5′ end and an Xho I site on the 3′ end. These sites were used for cloning of the tetramers into the X-GUS-90 vector, as described in the text. Construct 1, X-GUS-90; construct 2, 4II-90; construct 3, 4IIm-90; construct 4, 4AS1-90; construct 5, AS1m-90; WT, nontransformed tobacco. Each dot represents the activity of an independent transgenic plant.

Laboratory of Plant Molecular Biology, Rockefeller University, New York, NY 10021.

*To whom correspondence should be addressed at: AgBiotech Center, Waksman Institute of Microbiology, Rutgers State University, Piscataway, NJ 08855.